

Use of Resonance Energy Transfer To Study the Kinetics of Amphiphile Transfer between Vesicles[†]

J. Wylie Nichols and Richard E. Pagano*

ABSTRACT: Resonance energy transfer between 7-nitro-2,1,3-benzoxadiazol-4-yl (NBD) acyl chain labeled lipids (the energy donors) and (lissamine) Rhodamine B labeled phosphatidylethanolamine (*N*-Rh-PE) (energy acceptor) was used to monitor the rate of transfer of NBD-labeled lipids between two populations of small vesicles. When both fluorescent lipid analogues were incorporated into the same donor vesicle at ~1 mol %, NBD fluorescence was quenched by the *N*-Rh-PE due to resonance energy transfer. Addition of nonfluorescent acceptor vesicles to these donor vesicles resulted in an immediate and continuous change in NBD fluorescence due to the transfer of the NBD lipids, but not the nonexchangeable *N*-Rh-PE [Pagano, R. E., Martin, O. C., Schroit, A. J., & Struck, D. K. (1981) *Biochemistry* 20, 4920-4927], to the acceptor vesicles. Thus by continuously monitoring NBD fluorescence intensity, both the rate of transfer and equilibrium distribution of NBD-labeled lipids could be determined. Using

this technique, we found that the kinetics of transfer of NBD-labeled lipids were accurately predicted by a model based on the diffusion of soluble monomers as a function of both the acceptor and donor vesicle concentrations and the respective on-rate, off-rate, and affinity constants. By application of this model, we demonstrated that these rate constants for a given amphiphile depended on the structure of both its polar and nonpolar regions and on the lipid composition of the vesicle. In addition, when two vesicle populations had different off-rates for a given amphiphile, the half-time for equilibration was dependent on their concentration ratio. For the special case when acceptor vesicles were in excess, the half-time was solely dependent on the off-rate from the donor vesicles, and when the donor vesicles were in excess, the half-time was solely dependent on the off-rate from the acceptor vesicles.

BBiologically important amphiphilic molecules such as phospholipids, fatty acids, and cholesterol can be passively transferred between various combinations of vesicles, lipoproteins, and cellular membranes as soluble monomers diffusing through the aqueous medium (Duckwitz-Peterlein et al., 1977; Duckwitz-Peterlein & Moraal, 1978; Smith & Scow, 1979; Doody et al., 1980; Phillips et al., 1980; Roseman & Thompson, 1980; DeCuyper et al., 1980; McLean & Phillips, 1981). We recently reported the use of a fluorescently labeled phospholipid (C_{12} -NBD-PC)¹ to investigate the mechanism of amphiphile transfer between two populations of vesicles (Nichols & Pagano, 1981), where the C_{12} -NBD-PC transfer was monitored as it moved from donor vesicles containing self-quenching concentrations of this fluorescent molecule into unlabeled acceptor vesicles. Kinetic measurements of initial transfer rates indicated that transfer of this molecule occurs via the diffusion of soluble monomers.

In the present paper we present further studies of soluble monomer diffusion using resonance energy transfer to monitor the movement of fluorescent phospholipids between vesicles. This technique differs from that used in our earlier study since it allows continuous measurement of the transfer of probe molecules between vesicles. Furthermore, since the probes comprise only a small fraction of the total vesicle phospholipid, the equilibration of the fluorescent phospholipid molecules is not likely to result in significant perturbation of the bilayer structure of the donor and acceptor vesicles. Consequently, both rate and equilibrium measurements are possible. By combining the information gained from both rate and equilibrium measurements, we can determine the effect of the amphiphile structure and the vesicle composition on both the

rate at which the amphiphile enters and leaves the vesicle bilayer as well as the affinity of the amphiphile for vesicles of a given phospholipid composition.

Experimental Procedures

Materials and Routine Procedures. DOPC and BPS were purchased from Avanti Biochemical Corp., Birmingham, AL. EPC was purchased from Makor Chemicals Ltd., Jerusalem, Israel. [³H]DOPC was synthesized as described (Pagano et al., 1981b). Phospholipase D (cabbage) was obtained from Boehringer-Mannheim. Lipids were stored at -20 °C, periodically monitored for purity by thin-layer chromatography, and repurified when necessary. The concentrations of all phospholipids were determined by using a lipid phosphorus assay (Ames & Dubin, 1960). Radioactivity was measured with a Packard Tri-Carb liquid scintillation counter using a toluene-based scintillation fluid.

¹ Abbreviations: DOPC, dioleoylphosphatidylcholine; DPPC, dipalmitoylphosphatidylcholine; EPC, egg phosphatidylcholine; BPS, brain phosphatidylserine; Chol, cholesterol; NaCl-Hepes, 0.9% NaCl in 10 mM 4-(2-hydroxyethyl)-1-piperazineethanesulfonic acid, pH 7.4; NBD, 7-nitro-2,1,3-benzoxadiazol-4-yl; P- C_6 -NBD-PC, 1-palmitoyl-2-[6-[(7-nitro-2,1,3-benzoxadiazol-4-yl)amino]caproyl]phosphatidylcholine; P- C_6 -NBD-PA, 1-palmitoyl-2-[6-[(7-nitro-2,1,3-benzoxadiazol-4-yl)amino]caproyl]phosphatidic acid; P- C_6 -NBD-POA, 4-palmitoyl-3-[6-[(7-nitro-2,1,3-benzoxadiazol-4-yl)amino]caproyl]oxybutyl-1-phosphonic acid; C_6 -NBD-PC, 1-acyl-2-[6-[(7-nitro-2,1,3-benzoxadiazol-4-yl)amino]caproyl]phosphatidylcholine; C_6 -NBD-PA, 1-acyl-2-[6-[(7-nitro-2,1,3-benzoxadiazol-4-yl)amino]caproyl]phosphatidic acid; C_6 -NBD-PE, 1-acyl-2-[6-[(7-nitro-2,1,3-benzoxadiazol-4-yl)amino]caproyl]phosphatidylethanolamine; C_6 -NBD-PG, 1-acyl-2-[6-[(7-nitro-2,1,3-benzoxadiazol-4-yl)amino]caproyl]phosphatidylglycerol; C_6 -NBD-DG, 1-acyl-2-[6-[(7-nitro-2,1,3-benzoxadiazol-4-yl)amino]caproyl]diglyceride; C_{12} -NBD-PC, 1-acyl-2-[12-[(7-nitro-2,1,3-benzoxadiazol-4-yl)amino]dodecanoyl]phosphatidylcholine; C_{12} -NBD-PA, 1-acyl-2-[12-[(7-nitro-2,1,3-benzoxadiazol-4-yl)amino]dodecanoyl]phosphatidic acid; C_{12} -NBD-DG, 1-acyl-2-[12-[(7-nitro-2,1,3-benzoxadiazol-4-yl)amino]dodecanoyl]diglyceride; *N*-Rh-PE, *N*-(lissamine Rhodamine B sulfonyl)-dioleoylphosphatidylethanolamine.

[†] From the Department of Embryology, Carnegie Institution of Washington, Baltimore, Maryland 21210. Received September 11, 1981. This work was supported by the Carnegie Institution of Washington and U.S. Public Health Service Grant GM-22942. J.W.N. is a recipient of a National Institutes of Health postdoctoral fellowship.

Fluorescent Lipids. C₆-NBD-PC and P-C₆-NBD-PC (special order) were purchased from Avanti Biochemical Corp. P-C₆-NBD-PA, C₆-NBD-PA, C₆-NBD-PE, and C₆-NBD-PG were prepared from either P-C₆-NBD-PC or C₆-NBD-PC by using phospholipase D and the appropriate base (Comfurius & Zwaal, 1977) and were purified by thin-layer chromatography. P-C₆-NBD-POA was a gift from Dr. K. J. Longmair. N-Rh-PE was synthesized and purified as previously described (Struck et al., 1981).

Vesicle Preparation. Lipids were mixed in desired proportions and their storage solvents removed by evaporation under argon followed by overnight vacuum desiccation. Stock solutions of DOPC, EPC, and BPS contained known amounts of high specific activity [³H]DOPC for monitoring vesicle concentration. Vesicles containing EPC and BPS were prepared by ultrasonication as follows. Phospholipid dispersions (1.0 μmol/mL) in NaCl-Hepes were sonicated for 15 min at 10 °C under argon, centrifuged for 20 min at 12000g, and used on the same day as prepared. Vesicles containing DOPC were prepared by ethanol injection (Kremer et al., 1977) as follows. The dried phospholipids were dissolved in ethanol (5.0 μmol/mL), injected into NaCl-Hepes, and dialyzed against 4 L of NaCl-Hepes overnight at 4 °C. Additional dialysis against buffer to remove any remaining ethanol had no significant effect on the measured rates of transfer. The resulting vesicles (final concentration 250 nmol/mL) were used on the day following injection. Final concentrations of donor and acceptor carrier phospholipids were determined by liquid scintillation counting. Donor vesicles contained ~1 mol % NBD-labeled lipid and ~1 mol % N-Rh-PE, while acceptor vesicles contained no fluorescent lipids.

Fluorescence Measurements. Fluorescence was measured with an Aminco-Bowman spectrofluorometer equipped with crossed polarizers to reduce light scattering and was continuously recorded on a chart recorder. The excitation and emission slits were 1 mm. Peak absorbance of samples was kept to <0.1 to reduce inner filter effects. Solutions in the cuvette were continuously stirred by a pulsating jet of buffer, and the temperature was controlled by a circulating water bath. Concentrations of NBD-labeled lipids and N-Rh-PE in population I (donor) vesicles were obtained by disrupting the vesicles with Triton X-100 (1% final concentration). This treatment eliminated energy transfer and allowed the determination of the concentrations of NBD-labeled lipids and N-Rh-PE from their emission intensities by using direct excitation. The fluorescence yield per concentration of NBD-labeled lipids in the absence of N-Rh-PE (f_{I1} ; see eq 3) was obtained for EPC, BPS, and DOPC vesicles at 20 °C as follows. Vesicles were prepared containing a non-self-quenching concentration of NBD-labeled lipid (~0.2 mol %; Nichols & Pagano, 1981). NBD fluorescence emission intensity was measured by direct excitation, and the NBD concentration was determined after Triton X-100 disruption of the vesicles.

Use of Resonance Energy Transfer To Measure the Transfer of NBD-Labeled Lipids between Vesicles. The method used for measuring the rate of transfer and equilibrium distribution of NBD-labeled lipid between two populations of vesicles is shown in Figure 1. There is a significant overlap between the emission band of NBD and the excitation band of rhodamine such that these two fluorophores are an efficient donor-acceptor pair for resonance energy transfer (Struck et al., 1981). At the probe concentrations used in the donor vesicles in these experiments, this energy transfer resulted in quenching (>70%) of the NBD fluorescence (λ_{ex} 475 nm; λ_{em}

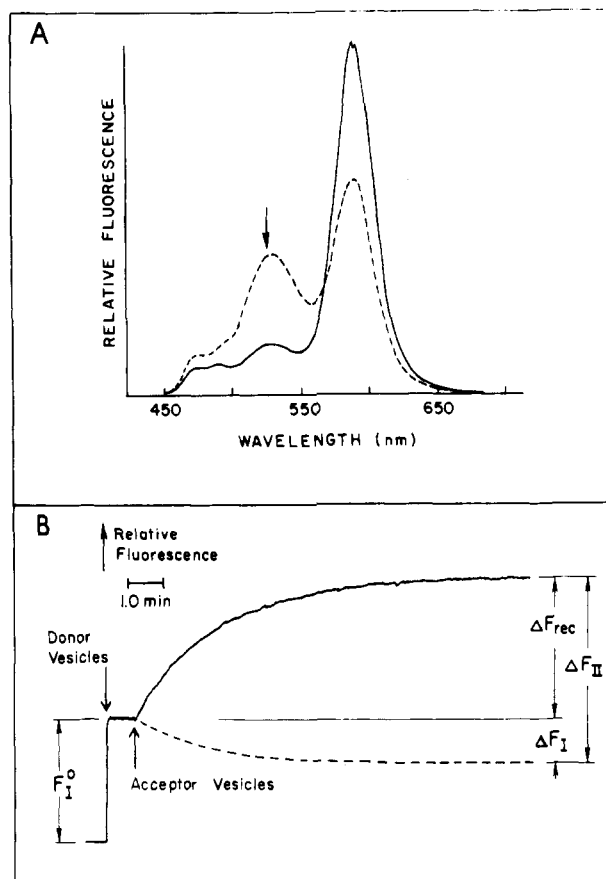


FIGURE 1: Use of resonance energy transfer to measure the kinetics of NBD-labeled lipid transfer between vesicles. (A) Emission spectra before and after transfer of P-C₆-NBD-PC. Emission spectrum (λ_{ex} 475 nm) of donor vesicles (—). Emission spectrum after addition of an approximately equal concentration of BPS vesicles (---). Arrow indicates emission wavelength monitored for rate measurements. (B) Kinetic measurement of P-C₆-NBD-PC transfer between BPS vesicles. Donor vesicles (1.16 μmol of total phospholipid/mL) composed of BPS/P-C₆-NBD-PC/N-Rh-PE (98.9:0.6:0.5 mol %) were added to NaCl-Hepes and allowed to equilibrate in the fluorometer at 20 °C. Fluorescence was recorded at 525 nm (λ_{ex} 475 nm). At time zero, acceptor vesicles containing 1.32 μmol of BPS/mL were added. Final concentrations of phospholipid in a total of 1.5 mL of NaCl-Hepes were the following: donor vesicles, 79.0 nmol/mL; acceptor vesicles, 79.0 nmol/mL. Vesicle suspensions were continuously stirred by a pulsating jet of buffer. See text for definition of parameters.

525 nm) and emission of rhodamine fluorescence (λ_{em} 590 nm) which would not normally be excited at 475 nm (Figure 1A, solid line).

Previous studies from this laboratory (Pagano et al., 1981b; Struck et al., 1981) have demonstrated that N-Rh-PE does not rapidly transfer between vesicles, while acyl chain labeled lipids, in general, transfer readily (Nichols & Pagano, 1981; Pagano et al., 1981b). Donor vesicles were mixed with non-fluorescent acceptor vesicles, and both the rate of transfer and equilibrium distribution of NBD-labeled lipid were determined from the change in NBD fluorescence intensity. The emission spectrum after equilibration of P-C₆-NBD-PC between the two vesicle populations (>10 min at 20 °C) (Figure 1A, dashed line) shows that the intensity of emitted light at the NBD peak increased and that of the rhodamine peak decreased due to a reduction in resonance energy transfer in the donor vesicles.

Figure 1B shows the time course of this process. Donor vesicles containing ~1 mol % NBD-labeled lipid and ~1 mol % N-Rh-PE were diluted in NaCl-Hepes and allowed to equilibrate to 20 °C, and at the indicated time, acceptor vesicles were added and the change in fluorescence was re-

corded. The fluorescence recorded in the donor (population I) vesicles prior to addition of acceptor vesicles (F_I^0) resulted from incomplete NBD quenching at the concentration of *N*-Rh-PE used in these studies. Upon addition of acceptor vesicles, an increase in fluorescence (ΔF_{rec}) was recorded with time which represented the sum of two processes: an increase as NBD-labeled phospholipids entered the acceptor (population II) vesicles (ΔF_{II}), where they were no longer quenched by *N*-Rh-PE, and a decrease resulting from the loss of NBD-labeled phospholipids from the donor (population I) vesicles (ΔF_I) (Figure 1A), or

$$\Delta F_{\text{rec}} = \Delta F_{\text{II}} - \Delta F_I \quad (1)$$

Since *N*-Rh-PE remained at a constant concentration in the donor vesicle, and since the efficiency of resonance energy transfer depends solely on the concentration of the energy acceptor (Stryer, 1978), the NBD fluorescence in the donor vesicles was directly proportional to its concentration in these vesicles. Therefore, the initial fluorescence in the donor vesicle (F_I^0) decreased by the same fraction of the total NBD-labeled phospholipid that is gained in the acceptor vesicles:

$$\Delta F_I = F_I^0 ([D]_{\text{II}} / [D]_I^T) \quad (2)$$

where $[D]_{\text{II}}$ is the concentration in bulk solution of NBD-labeled phospholipid in population II at a given time and $[D]_I^T$ is the total concentration in bulk solution of NBD-labeled phospholipid initially in population I. If f_{II} is the fluorescence yield per bulk solution concentration of NBD-labeled phospholipid in population II vesicles, then

$$[D]_{\text{II}} = \Delta F_{\text{II}} / f_{\text{II}} \quad (3)$$

Equations 1–3 can be solved algebraically for $[D]_{\text{II}}$:

$$[D]_{\text{II}} = \Delta F_{\text{rec}} / (f_{\text{II}} - F_I^0 / [D]_I^T) \quad (4)$$

Since ΔF_{rec} is related to $[D]_{\text{II}}$ by a constant term for a given experiment (eq 4), the half-time for ΔF_{rec} and $[D]_{\text{II}}$ to reach equilibrium is equal (see eq A9–A11 in the Appendix). Therefore, the half-time for $[D]_{\text{II}}$ to reach equilibrium could be measured directly from the recorded fluorescence trace.

Determination of Vesicle On-Rate, Off-Rate, and Affinity Constants. Since acyl chain labeled NBD phospholipid transfer between vesicles occurs via the diffusion of soluble monomers (see Results), eq A11 and A14 in the Appendix predict the dependence of the half-time for equilibration and the equilibrium distribution on the ratio of donor to acceptor vesicle concentrations. These equations can therefore be used to determine the kinetic rate and affinity constants for this process. For the special case where the phospholipid composition of the donor vesicles (population I) is the same as that of the acceptor vesicles (population II), the half-time for equilibration of the NBD-labeled phospholipid is independent of the ratio of the surface areas. This condition was used to determine the off-rate constants for a given probe molecule and a given phospholipid vesicle.

When the ratio of the total amount of NBD-labeled phospholipid to the amount transferred to the acceptor vesicle at equilibrium ($[D]_I^T / [D]_{\text{II}}^{\text{eq}}$) is plotted vs. the ratio of the donor to acceptor external surface areas $[s_A[A]_I] / [s_B[B]_{\text{II}}]$, eq A14 predicts a straight line. The y intercept of this line is equal to the inverse of the fraction of the total amount of NBD-labeled phospholipid initially contained in population I that is available for transfer (α_D^{-1}). The slope of this line divided by the y intercept equals the ratio of the probe affinity for the donor to acceptor vesicles. Since there is no dependable method for measuring the actual external surface areas of the two vesicle populations, we have estimated this value by assuming similar size dispersions in the two populations and using

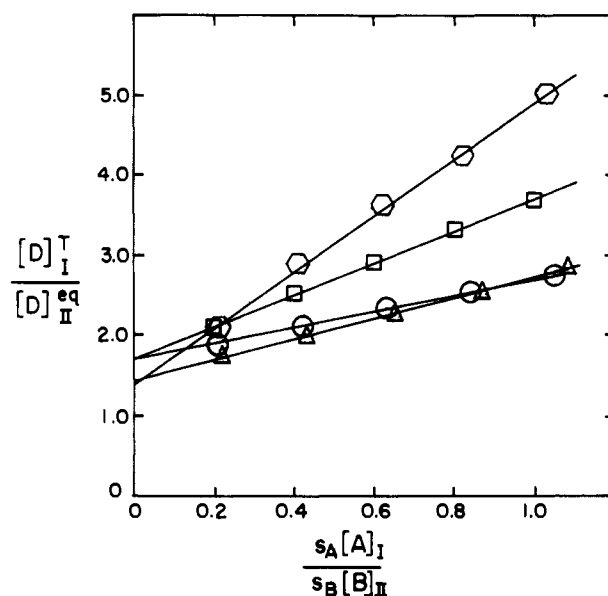


FIGURE 2: Comparison of P-C₆-NBD-PC transfer between EPC and BPS vesicles. Plot of the ratio of total NBD lipid concentration to that in acceptor vesicles at equilibrium vs. the ratio of donor to acceptor external surface areas (refer to eq A14). Symbols are defined in Table I. Experiments were performed at 20 °C. s_{EPC} was estimated to be 81 Å²/molecule (Tinoco & McIntosh, 1970) and s_{BPS} , 70 Å²/molecule (Papahadjopoulos, 1968).

literature values for the molecular surface areas of the lipids being compared. The molecular surface areas for EPC and BPS were obtained from packing densities of surface films by using the arbitrary value of 20 dyn/cm surface pressure (Tinoco & McIntosh, 1970; Papahadjopoulos, 1968). Since the affinity constant is defined as the ratio of the on- to off-rate constants, the ratio of the on-rate constants for two different vesicle compositions can be calculated by multiplying the affinity constant ratio by the ratio of the off-rate constants (see Appendix).

Results

Diffusion- vs. Collision-Mediated Transfer. The transfer of lipid molecules between vesicles via the diffusion of soluble monomers can be kinetically distinguished from transfer resulting from vesicle collision. The half-time for equilibration of a diffusion-mediated process is predicted to remain constant as the donor and acceptor vesicle concentrations are increased proportionately (see eq A11), whereas the half-time for a collision-mediated process will decrease hyperbolically.² In experiments designed to test these predictions, the half-time for equilibration remained constant (data not shown). Consistent with our previous studies (Nichols & Pagano, 1981), this result indicates that NBD-labeled lipids are transferred as soluble monomers.

Comparison of P-C₆-NBD-PC Transfer between EPC and BPS Vesicles. The results of a series of experiments measuring the equilibrium distribution of the neutral zwitterion, P-C₆-NBD-PC, between charged BPS and uncharged EPC vesicles are presented in Figure 2. These data are plotted according to eq A14, and the results are presented in the upper half of Table I and are compiled in Table II. The inverse of the y

² The derivation of the equilibration rate equation based on collision-mediated transfer is not included but was derived in an analogous manner to the diffusion-mediated model. The rate at which an amphiphile transfers between two populations of vesicles was assumed to be proportional to the fraction of the external surface it occupies multiplied by the product of the number of vesicles in each population.

Table I: Constants Derived from Figures 2-4

figure	symbol	donor vesicle composition (I)	acceptor vesicle composition (II)	α_D^{Ia}	$\frac{K_D^{Ia}}{K_D^{II}}$	$t_{1/2}$ (min)
Lipid:P-C ₆ -NBD-PC						
2	□	egg PC	egg PC	0.59	1.17	0.41 ± 0.03
2	○	egg PC	brain PS	0.59	0.59	
2	△	brain PS	brain PS	0.69	0.91	1.42 ± 0.08
2	○	brain PS	egg PC	0.72	2.55	
Lipid:P-C ₆ -NBD-PA						
3	□	egg PC	egg PC	0.47	1.01	0.25 ± 0.02
3	○	egg PC	brain PS	0.52	2.81	
3	△	brain PS	brain PS	0.59	1.04	0.38 ± 0.02
3	○	brain PS	egg PC	0.61	0.36	

^a α_D^I is the fraction of the total concentration of D lipid that is available for transfer. K_D^I/K_D^{II} is the ratio of the D lipid affinity for population I and population II vesicles. Half-times are presented ± the standard deviation for five trials.

Table II: Compilation of Constants Presented in Table I

probe	temp (°C)	vesicle composition (I)	vesicle composition (II)	α_D^{Ia}	α_D^{IIa}	k_{D-}^{Ib}	k_{D-}^{IIb}	$\frac{K_D^I}{K_D^{IIc}}$	$\frac{k_{D-}^I}{k_{D-}^{II}}$	$\frac{k_{D+}^I}{k_{D+}^{IId}}$
P-C ₆ -NBD-PC	20	EPC	BPS	0.59	0.70	1.67	0.49	0.5	3.4	1.7
P-C ₆ -NBD-PA	20	EPC	BPS	0.49	0.60	2.73	1.82	2.8	1.5	4.2

^a Two values of α_D^I for each donor vesicle from Table I were averaged. ^b The half-times for homologous donors and acceptors from Table I were substituted into eq A12 to calculate the off-rate constant. ^c The two values for the affinity constant ratio for vesicle composition I and vesicle composition II were averaged. For example, the affinity constant ratio obtained when EPC vesicles were used as donors and BPS vesicles as acceptors was averaged with the inverse of the ratio obtained when BPS vesicles were used as donors and EPC vesicles as acceptors. ^d The ratio of on-rates was obtained by multiplying the affinity constant ratio by the ratio of off-rates.

intercepts of the lines plotted in Figure 2 equals the fraction of the total amount of NBD-labeled phospholipid initially in the donor vesicles that is in equilibrium with the acceptor vesicles (α_D^I). The values of the y intercepts in Figure 2 are similar for identical donor vesicles but differ slightly between the two different donor types ($\alpha_D^{EPC} = 0.59$, $\alpha_D^{BPS} = 0.70$). We interpret these fractions to represent the distribution of probe between the inner and outer leaflets of the donor vesicle bilayers. Once the probe has equilibrated between donor and acceptor vesicles, there is no detectable increase in fluorescence on the time scale used for these measurements. This indicates that transverse bilayer movement or "flip-flop" of the probe occurs very slowly if at all. The value for α_D^I is consistent with a random distribution of the probe molecules between the inner and outer leaflets of small unilamellar vesicles (Johnson et al., 1975; Rothman & Dawidowicz, 1975; DiCorleto & Zilversmit, 1977). The slight increase in P-C₆-NBD-PC molecules in the outer leaflet of BPS vesicles as compared to EPC vesicles could result from a size difference in the two populations (BPS vesicles being smaller than EPC vesicles), or the probe may be partitioned preferentially into the outer leaflet of BPS vesicles.

The results compiled in Table II indicate that the P-C₆-NBD-PC off-rate from EPC vesicles is 3.4 times greater than that from BPS vesicles, and its on-rate is only 1.7 times greater for EPC than for BPS vesicles. The net result is a 2-fold decrease in the probe affinity for EPC when compared to BPS vesicles.

Comparison of P-C₆-NBD-PA Transfer between EPC and BPS Vesicles. The results of a series of experiments measuring the equilibrium distribution of the negatively charged probe, P-C₆-NBD-PA, between charged BPS vesicles and uncharged EPC vesicles are presented in Figure 3 and in Tables I and II. The value of α_D^I is 0.60 for BPS vesicles and 0.49 for the EPC vesicles, indicating a random distribution of the negatively charged probe in the negatively charged vesicles and a slight preference for the inner leaflet in the neutral vesicles. A similar asymmetric distribution of small percentages of negatively

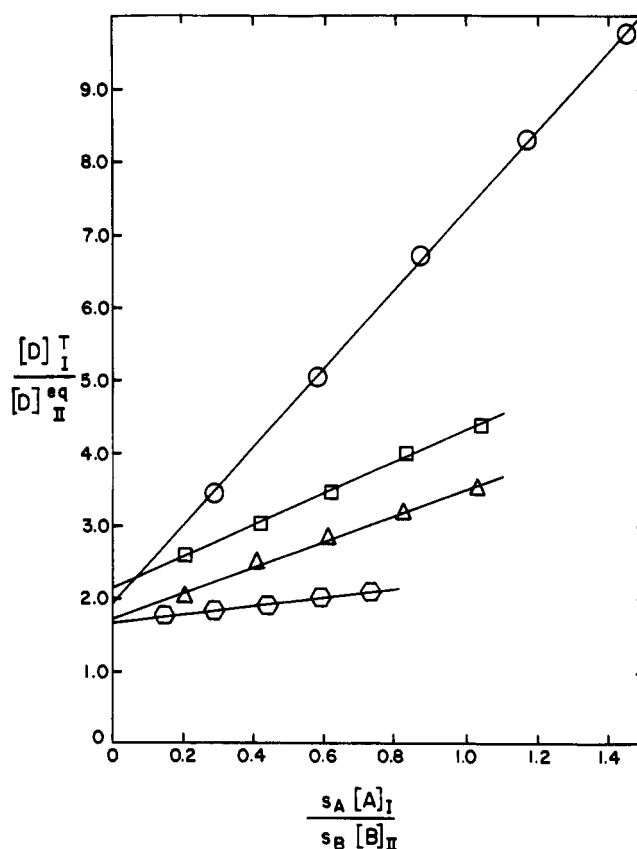


FIGURE 3: Comparison of P-C₆-NBD-PA transfer between EPC and BPS vesicles. Plot of eq A14. Symbols are defined in Table I. Experiments were performed at 20 °C. s_{EPC} and s_{BPS} were estimated as described in the legend to Figure 2.

charged phospholipids contained in phosphatidylcholine vesicles has been shown previously (Litman, 1973, 1974; Berden et al., 1975; Barsukov et al., 1980).

The results compiled in Table II indicate that the P-C₆-NBD-PA off-rate from EPC vesicles is 1.5 times greater than

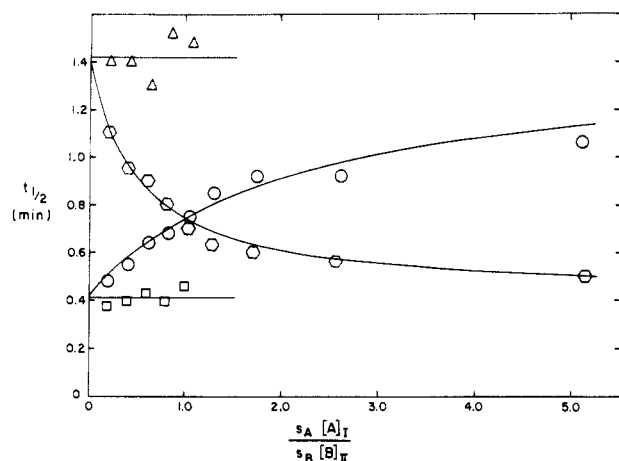


FIGURE 4: Plot of half-time for equilibration of P-C₆-NBD-PC vs. the ratio of donor to acceptor external surface area. Donor and acceptor vesicles were identical with those used in Figure 2. The symbols are defined in Table I and represent the measured half-time for the experiments presented in Figure 2. For donor to acceptor surface area ratios less than 1, the acceptor concentration was held constant while the donor concentration was varied. For donor to acceptor surface area ratios greater than 1, the donor concentration was held constant while the acceptor concentration was varied.

that from BPS vesicles, and its on-rate is 4.2 times greater for EPC than for BPS vesicles. The net result is a 2.8-fold increase in the probe affinity for EPC compared to BPS vesicles.

Measurement of Half-Time for Equilibration of P-C₆-NBD-PC between EPC and BPS Vesicles. The half-time for P-C₆-NBD-PC equilibration vs. the ratio of the external surface areas is plotted in Figure 4. This plot demonstrates the relationship of these two variables as predicted by eq A11 and illustrates two special cases. As described in the Appendix, when donors and acceptors are composed of the same lipids, eq A11 reduces to eq A12, and $t_{1/2}$ is independent of the donor and acceptor surface area ratio. This independence is clearly seen in the upper and lower lines of Figure 4 where there is virtually no change in $t_{1/2}$ over a 5-fold change in the ratio of donor to acceptor surface areas. When the donors and acceptors with different off-rates are mixed, the equilibration half-times are intermediate between the half-times measured for homologous donors and acceptors. In addition, these plots illustrate a second special case of eq A11. As the donor to acceptor surface area ratio approaches zero, eq A11 reduces to eq A12, and the half-time is predicted to approach that measured for the donor vesicles with homologous vesicles. Conversely, as the donor to acceptor surface area ratio approaches infinity, the half-time is predicted to approach that measured for the acceptor vesicles with homologous vesicles. The solid curved lines in Figure 4 were projected for the heterologous vesicle experiments from eq A11 by using the off-rate and affinity ratios from Table II. This projected curve accurately predicts the measured half-time dependence on external surface area ratio. We conclude that the half-time for diffusion-mediated equilibration between two populations of vesicles having different off-rates varies with the ratio of their surface areas. When acceptors are in excess, the half-time is determined by the donor off-rate, and when donors are in excess, the half-time is determined by the acceptor off-rate.

Effect of Head Group and Acyl Chain Length on the Off-Rates for NBD Phospholipids from DOPC Vesicles. As discussed previously, when both the donor and acceptor vesicles are of the same phospholipid composition, $k_D^I = k_D^{II}$ such that eq A11 reduces to $t_{1/2} = (\ln 2)/k_D^I$. Therefore, measurements of the half-time of equilibration will reflect the off-rate constant for a given type of phospholipid vesicle. Using

Table III: Effect of Head-Group Moiety on the Off-Rate Constant in DOPC Vesicles^a

probe	$t_{1/2}$ (min)	k_D^I (min ⁻¹)
C ₆ -NBD-PA	0.55	1.26
C ₆ -NBD-PC	0.78	0.89
P-C ₆ -NBD-POA	1.00	0.69
C ₆ -NBD-PG	1.26	0.55
C ₆ -NBD-PE	1.54	0.45
C ₆ -NBD-DG	34.0	0.020
C ₁₂ -NBD-PA	125.0	5.5×10^{-3}
C ₁₂ -NBD-PC	150.0	4.6×10^{-3}
C ₁₂ -NBD-DG	>2000.0	3.5×10^{-4}

^a Equilibration rate measurements were made between donor vesicles containing approximately 1.0% of the NBD-labeled probe, 1.0% N-Rh-PE, and 98% DOPC and acceptor vesicles containing only DOPC.

these conditions, we have compared the effect of the head-group composition and length of the acyl chains on the off-rates from DOPC vesicles (Table III). The order of NBD-labeled lipids according to their rate of equilibration is C₆-NBD-PA > PC > PG > PE >> DG. For a given acyl chain composition, changes in the polar head group result in minimal differences in off-rates (1–3-fold) with the exception that the diacylglyceride off-rate constant is decreased over 20-fold. The use of C₁₂-NBD in place of C₆-NBD results in a very large decrease in the off-rate for the same head group. Note that the ratio of off-rates for C₆-NBD-PA to C₆-NBD-PC (1.42) is similar to the ratio for C₁₂-NBD-PA to C₁₂-NBD-PC (1.20), indicating a consistent effect of the polar head group on the off-rate regardless of the acyl chain length.

Discussion

We have presented several examples illustrating the relationship of the on- and off-rate constants for fluorescent phospholipid analogues diffusing between phospholipid vesicles. In the first case presented (Figure 2), P-C₆-NBD-PC is 1.7 times more likely to enter and 3.4 times more likely to leave an EPC vesicle than a BPS vesicle (Table II). In this case the difference in off-rates predominates, decreasing both P-C₆-NBD-PC affinity for and concentration in the EPC vesicles as compared to BPS vesicles. The 3.4-fold difference in off-rates may result from small differences in the acyl chain composition between EPC and BPS vesicles but more likely results from the large difference in surface charge density between the two. For whatever reason, the net result is a 2-fold greater P-C₆-NBD-PC affinity for BPS than for EPC vesicles.

Conversely, the negatively charged probe, P-C₆-NBD-PA, has a 2.8 times higher affinity for EPC than for BPS vesicles (Figure 3 and Table II). The on-rate for EPC vesicles is 4.2 times and the off-rate is 1.5 times greater for EPC than for BPS vesicles. If electrostatic charge repulsion between the negatively charged probe molecule and the negative surface of the BPS vesicle were solely responsible for these differences in on- and off-rates, one would predict that the on-rate into BPS vesicles would decrease relative to EPC vesicles and the off-rate would increase. Our results do not confirm this prediction but rather suggest that some other interaction in addition to charge repulsion between the probe and vesicles is affecting the rate constants.

In summary, we have presented a model that predicts the kinetics of transfer of soluble monomer diffusion between vesicles and have demonstrated that the affinity and rate constants for this type of transfer are dependent on the properties of both the amphiphile and the vesicle bilayer. Furthermore, the on- and off-rate constants can vary independently of each other to determine the affinity of an am-

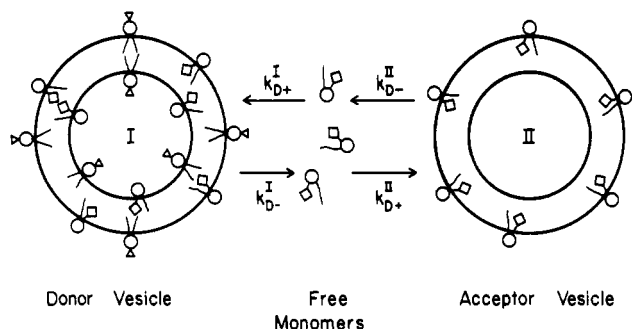


FIGURE A1: Schematic diagram of diffusion-mediated transfer process and definition of rate constants.

phiphile for a given membrane. For different membranes having differing off-rate constants for a given amphiphile, the half-time for equilibration of this amphiphile is not a constant but instead will vary depending on the surface area ratio of the two membranes. We recognize that because of the altered structure imposed upon these phospholipids by the attachment of a fluorescent label, the transfer rates of naturally occurring phospholipids cannot be directly inferred from our studies. However, the relative ease with which transfer measurements can be made with these probes makes them ideally suited to study the general principles governing the diffusion of soluble monomers. Our hope is that these principles will prove generally useful in understanding passive diffusion of biologically relevant amphiphiles between membranes. In addition, this work provides important background information for our studies of the metabolism and translocation of these lipid analogues in cultured cells (Pagano et al., 1981a).

Acknowledgments

We thank Susan Satchell and Pat Schmidt for the preparation of the manuscript and Ona Martin for expert technical assistance.

Appendix

Diffusion-Mediated Model. Rate equations for the diffusion-mediated model (Nakagawa, 1974; Thilo, 1977; Nichols & Pagano, 1981) can be written by assuming that the rate at which an amphiphile monomer escapes from the surface of a bilayer membrane is proportional to its concentration on that surface and that the adsorption rate is proportional to the product of the free monomer concentration and the surface area of the membrane (Figure A1). By use of these predictions the following rate equations describing the transfer of the amphiphilic probe molecule D between two populations of vesicles composed of phospholipid A and B can be written:

$$\frac{d[D]_I}{dt} = k_{D+}^I[D]_m(s_D[D]_I + s_A[A]_I) - k_{D-}^I[D]_I \quad (A1)$$

$$\frac{d[D]_{II}}{dt} = k_{D+}^{II}[D]_m(s_D[D]_{II} + s_B[B]_{II}) - k_{D-}^{II}[D]_{II} \quad (A2)$$

k_{D+}^I and k_{D+}^{II} are the on-rate constants of the D lipid into vesicle populations I and II, respectively. k_{D-}^I and k_{D-}^{II} are the corresponding off-rate constants. $[D]_m$ is the free monomer concentration of the D lipid and $[D]_I$, $[D]_{II}$, $[A]_I$, and $[B]_{II}$ are the concentrations of the D, A, and B lipids exposed to the bulk solution in the subscripted vesicle populations. s_A , s_B , and s_D are the surface area per mole of the subscripted lipid.

At steady-state equilibrium

$$\frac{d[D]_I}{dt} + \frac{d[D]_{II}}{dt} = 0 \quad (A3)$$

Substituting eq 1 and 2 and solving for $[D]_m$

$$[D]_m = \frac{k_{D-}^I[D]_I + k_{D-}^{II}[D]_{II}}{k_{D+}^I(s_D[D]_I + s_A[A]_I) + k_{D+}^{II}(s_D[D]_{II} + s_B[B]_{II})} \quad (A4)$$

With the assumption that steady-state equilibrium is reached quickly in relation to the transfer process, eq A4 can be substituted into eq A2 such that

$$\frac{d[D]_{II}}{dt} = \frac{k_{D+}^{II}(k_{D-}^I[D]_I + k_{D-}^{II}[D]_{II})(s_D[D]_{II} + s_B[B]_{II})}{k_{D+}^I(s_D[D]_I + s_A[A]_I) + k_{D+}^{II}(s_D[D]_{II} + s_B[B]_{II})} - k_{D-}^{II}[D]_{II} \quad (A5)$$

For the special case which is often used in studies of lipid transport, where the donor and acceptor vesicles are composed of the same phospholipid and the acceptor vesicle concentration is in excess of the donor, eq A5 reduces to

$$\frac{d[D]_{II}}{dt} = k_{D-}^I[D]_I \quad (A6)$$

Equation A5 can be integrated if the following assumptions and substitutions are made. If probe D transfers more rapidly than phospholipids A and B, they can be assumed to remain constant during the time required for D equilibration. If $[D]_I$ and $[D]_{II}$ are a small fraction of $[A]_I$ and $[B]_{II}$, then

$$\begin{aligned} s_D[D]_I + s_A[A]_I &\approx s_A[A]_I \\ s_D[D]_{II} + s_B[B]_{II} &\approx s_B[B]_{II} \end{aligned} \quad (A7)$$

If initially only population I contains the D lipid and trans-bilayer transfer or flip-flop is slow relative to the transfer process, then

$$\alpha_D^I[D]_I^T = [D]_I + [D]_{II} \quad (A8)$$

where $[D]_I^T$ is the total concentration of D in vesicle population I initially and α_D^I is the fraction of the total D that is exposed to the external solution. After the above substitutions are made, eq A5 can be integrated to give

$$[D]_{II} = \frac{\alpha_D^I[D]_I^T}{1 + \frac{s_A k_{D+}^I k_{D-}^{II}[A]_I}{s_B k_{D+}^{II} k_{D-}^I[B]_{II}}} - \frac{\alpha_D^I[D]_I^T}{1 + \frac{s_A k_{D+}^I k_{D-}^{II}[A]_I}{s_B k_{D+}^{II} k_{D-}^I[B]_{II}}} \times \left[\exp\left(-\frac{s_B k_{D+}^{II} k_{D-}^I[B]_{II} + s_A k_{D+}^I k_{D-}^{II}[A]_I}{s_A k_{D+}^I[A]_{II} + s_B k_{D+}^{II}[B]_{II}}\right)t \right] \quad (A9)$$

The half-time for $[D]_{II}$ to reach equilibrium is therefore

$$t_{1/2} = \frac{(\ln 2) \left(s_A[A]_I + s_B \frac{k_{D+}^{II}}{k_{D+}^I}[B]_{II} \right)}{\frac{k_{D+}^{II}}{s_B k_{D+}^I} k_{D-}^I[B]_{II} + s_A k_{D-}^{II}[A]_I} \quad (A10)$$

The affinity constant of the D probe for the population I vesicles, K_D^I , is defined as the ratio k_{D+}^I/k_{D-}^I , and K_D^{II} is defined similarly for population II vesicles. Substitution of these affinity constants for the rate constants results in eq A11:

$$t_{1/2} = \frac{(\ln 2) \left[\frac{s_A[A]_I}{s_B[B]_{II}} \left(\frac{1}{k_{D-}^{II}} \right) + \frac{K_D^{II}}{K_D^I} \left(\frac{1}{k_{D-}^I} \right) \right]}{\frac{K_D^{II}}{K_D^I} + \frac{s_A[A]_I}{s_B[B]_{II}}} \quad (A11)$$

For the special case where lipid A is the same as lipid B, then $k_{D-}^I = k_{D-}^{II}$, $k_{D+}^I = k_{D+}^{II}$, and $s_A = s_B$ such that

$$t_{1/2} = (\ln 2)/k_{D-}^I \quad (\text{A12})$$

At equilibrium, the exponential term in eq A9 approaches zero, such that

$$[D]_{II}^{eq} = \frac{\alpha_D^I [D]_I^T}{1 + \frac{s_A k_{D+}^I k_{D-}^{II} [A]_I}{s_B k_{D+}^{II} k_{D-}^I [B]_{II}}} \quad (\text{A13})$$

Substituting the affinity constant K for the ratio of the on- and off-rate constant and rearranging

$$\frac{[D]_I^T}{[D]_{II}^{eq}} = \frac{K_D^I s_A [A]_I}{\alpha_D^I K_D^{II} s_B [B]_{II}} + \frac{1}{\alpha_D^I} \quad (\text{A14})$$

A plot of $[D]_I^T/[D]_{II}^{eq}$ vs. $s_A[A]_I/(s_B[B]_{II})$ is predicted to be linear with the y intercept equal to α_D^I . The slope divided by the intercept equals the ratio of the probe affinity constants for the two vesicle types.

References

- Ames, B. N., & Dubin, D. T. (1960) *J. Biol. Chem.* 235, 769–775.
- Barsukov, L. I., Victorov, A. V., Vasilenko, I. A., Erstigneera, R. P., & Bergelson, L. D. (1980) *Biochim. Biophys. Acta* 598, 153–168.
- Berden, J. A., Barker, R. W., & Radda, G. K. (1975) *Biochim. Biophys. Acta* 375, 186–208.
- Comfurius, P., & Zwaal, R. F. A. (1977) *Biochim. Biophys. Acta* 488, 36–42.
- DeCuyper, M., Joniau, M., & Dangreau, H. (1980) *Biochem. Biophys. Res. Commun.* 95, 1224–1230.
- DiCorleto, P. E., & Zilversmit, D. B. (1977) *Biochemistry* 16, 2145–2150.
- Doody, M. C., Pownall, H. J., Kao, Y. J., & Smith, L. C. (1980) *Biochemistry* 19, 108–116.
- Duckwitz-Peterlein, G., & Moraal, H. (1978) *Biophys. Struct. Mech.* 4, 315–326.
- Duckwitz-Peterlein, G., Eilenberger, G., & Overath, P. (1977) *Biochim. Biophys. Acta* 469, 311–325.
- Johnson, L. W., Hughes, M. E., & Zilversmit, D. B. (1975) *Biochim. Biophys. Acta* 375, 176–185.
- Kremer, J. M. H., v.d. Esker, M. W. J., Pathmamanoharan, C., & Wiersema, P. H. (1977) *Biochemistry* 16, 3932–3935.
- Litman, B. J. (1973) *Biochemistry* 12, 2545–2554.
- Litman, B. J. (1974) *Biochemistry* 13, 2844–2848.
- McLean, L. R., & Phillips, M. C. (1981) *Biochemistry* 20, 2893–2900.
- Nakagawa, T. (1974) *Colloid Polym. Sci.* 252, 56–64.
- Nichols, J. W., & Pagano, R. E. (1981) *Biochemistry* 20, 2783–2789.
- Pagano, R. E., Longmuir, K. J., Martin, O. C., & Struck, D. K. (1981a) *J. Cell Biol.* 91, 872–877.
- Pagano, R. E., Martin, O. C., Schroit, A. J., & Struck, D. K. (1981b) *Biochemistry* 20, 4920–4927.
- Papahadjopoulos, D. (1968) *Biochim. Biophys. Acta* 163, 240–254.
- Phillips, M. C., McLean, L. R., Stoudt, G. W., & Rothblat, G. H. (1980) *Atherosclerosis (Shannon, Ireland)* 36, 409–422.
- Roseman, M. A., & Thompson, T. E. (1980) *Biochemistry* 19, 439–444.
- Rothman, J. E., & Dawidowicz, E. A. (1975) *Biochemistry* 14, 2809–2816.
- Smith, L. C., & Scow, R. O. (1979) *Prog. Biochem. Pharmacol.* 15, 109.
- Struck, D. K., Hoekstra, D., & Pagano, R. E. (1981) *Biochemistry* 20, 4093–4099.
- Stryer, L. (1978) *Annu. Rev. Biochem.* 47, 819–846.
- Thilo, L. (1977) *Biochim. Biophys. Acta* 469, 326–334.
- Tinoco, J., & McIntosh, D. J. (1970) *Chem. Phys. Lipids* 4, 72–84.